CARBON letters

Note

Carbon Letters Vol. 27, 112-116 (2018)

Electrochemical properties of KOH-activated lyocell-based carbon fibers for EDLCs

Jin-Young Jung[1] and Young-Seak Lee[2,♣]

[1]The 5th Research and Development Institute, Agency for Defense Development, Daejeon 34186, Korea
[2]Department of Chemical Engineering and Applied Chemistry, Chungnam National University, Daejeon 34134, Korea

Article Info

Received 12 March 2018
Accepted 27 March 2018

♣Corresponding Author
E-mail: youngslee@cnu.ac.kr
Tel: +82-42-821-7007

Open Access

DOI: http://dx.doi.org/10.5714/CL.2018.27.112

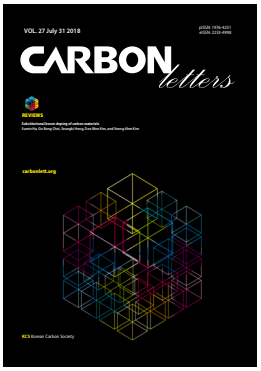

http://carbonlett.org

pISSN: 1976-4251
eISSN: 2233-4998

Electrochemical double-layer capacitors (EDLCs), which are generally known as super capacitors, have been considered as power sources in telecommunication devices, standby power systems, and portable electronic devices [1]. EDLCs are promising energy storage devices for applications that require longer lifecycles, higher power capabilities, exceptional cycle lifetimes, and high rate performance [2-5]. The capacitance of an EDLC depends on the surface area of the electrode materials. Thus, carbons materials with porous structures, such as activated carbon (AC) and carbon nanotubes, are attractive because of their large surface area, unique pore structure, good adsorption properties, and electrochemical stability [6-8]. The high specific surface area of AC is expected to endow EDLCs fabricated with AC with outstanding electrochemical performance. Developing AC materials with an appropriate surface area, pore size and shape is crucial for increasing their capacity. Researchers have attempted to control these aspects of AC materials, but AC material development is still challenging. In recent years, AC fibers have received attention for their potential applications. Their structural and electronic properties make them applicable as electrodes in EDLCs [9].

KOH chemical activation is an effective treatment used to prepare AC containing micropores with a homogeneous pore-size distribution [10]. Chemical activation leads to a higher yield and more porosity in comparison to physical activation processes, such as steam or carbon dioxide activation. Activated carbon fibers (ACFs) are commercially produced with low yield and low porosity by physical activation using carbon dioxide or steam. AC pores can be classified as micropores (<2 nm), mesopores (2–50 nm), and macropores (>50 nm) [11]. Micropores result in a high surface area, which is crucial for charging an electrical double layer and determining the capacitance value. In general, KOH activation leads to a higher specific surface area and larger pore volume than $ZnCl_2$ activation [12].

Lyocell fibers are 100% manmade cellulose fibers spun from wood or cotton pulp in a closed amine-oxide solvent system. They have attracted attention because of their environmentally friendly production process and unique fiber properties [13]. Additionally, these fibers have unique characteristics in different states, such as a higher tenacity and modulus in the dry state and a lower tenacity and modulus in the wet state [14]. Therefore, lyocell fibers are excellent precursors for creating high-performance carbon fibers.

In this work, we used lyocell fibers as precursors to prepare porous carbon fibers with a pore volume and micro-sized pore diameter suitable for EDLCs. To produce lyocell-based ACFs with a micropore structure, heat treatment and chemical activation were conducted using a KOH activating agent. The morphology, texture, and electrochemical properties of the prepared samples were investigated. The influence of the pore structure on the electrochemical properties was also examined.

The precursor of the lyocell-based carbon fibers (LCFs) used in this work was lyocell fibers supplied by the Kolon Company in Korea. KOH (potassium hydroxide, 95.0%; Samchun, Korea) was used as an activation agent to obtain the lyocell-based ACFs (LACFs). The electrodes were prepared by mixing 80 wt% ACFs, 10 wt% carbon black (Super P; Timcal Ltd., Switzerland), and 10 wt% polyvinyldine fluoride (PVDF; Aldrich, USA) in N-methyl pyrrolidone (NMP; Aldrich, USA) to obtain a slurry. The slurry was painted on a titanium plate. After drying the plate in an oven at 100°C, the resulting electrode was pressed at a pressure of 200 bars for 10 min at 150°C.

Lyocell fibers were stabilized at 250°C for 20 min under an air atmosphere in a furnace. After stabilization, the stabilized fibers were carbonized at 800°C for 1 h under a nitrogen atmosphere at a heating rate of 5°C/min. The heat-treated fibers were then cooled down to room temperature. KOH solutions (2, 4, and 6 M) were prepared for chemical activation. The carbon fibers were placed in an alumina boat in a furnace at a ratio of KOH solution/carbon fibers=20 mL g^{-1}. In addition, chemical activation was conducted at 700°C for 3 h in a nitrogen atmosphere. After chemical activation, the samples were washed with distilled water to remove residual potassium and dried in an oven at 100°C for 24 h. These ACFs were labeled as LCF, 2K-LACF, 4K-LACF and 6K-LACF according to the KOH concentrations (0, 2, 4 and 6 M, respectively).

To examine the surface morphology of the prepared LACFs, scanning electron microscope (SEM) images were obtained by sputter coating the samples with platinum using a field-emission scanning electron microscope (FE-SEM; S-5500, Hitachi, Japan). The nitrogen adsorption/desorption isotherms and the textural properties of the materials were determined by a conventional volumetric technique at 77 K using nitrogen with a Micromeritics ASAP 2020 (USA) volumetric adsorption apparatus. The Brunauer-Emmett-Teller (BET) specific surface area and pore volumes were calculated by BET surface analysis based on the adsorption data. The electrochemical properties of the prepared LACF-based electrode were examined by a Compacstat electrochemical interface (Ivium Technologies, The Netherlands) using a three-electrode assembly. The prepared LACF-based electrode was used as the working electrode, and Ag/AgCl and a platinum wire were used as the reference and counter electrodes, respectively. The electrochemical measurements were carried out in a 1 M H_2SO_4 electrolyte. Cyclic voltammetry (CV) of the electrode materials was performed over a potential range of 0 to 1 V.

Fig. 1 shows SEM images of the LCFs (Fig. 1a) and LACFs (Fig. 1b-d) prepared using various concentrations of KOH. The surfaces of the LCFs and LACFs were smooth and clear, as shown in Fig. 1. The average diameter of the heat-treated carbon fibers (Fig. 1a) was 7.26±0.1 μm and relatively uniform. Meanwhile, the effect of KOH activation on the morphology is presented in Fig. 1b-d. As the KOH concentration increased from 2 M to 6 M, the fiber diameter decreased by approximately 7% to 23% (2 M: 6.75±0.2 μm, 4 M: 6.38±0.3 μm, and 6 M: 5.62±0.1 μm) for the LCFs. The decrease in the fiber diameter may have been caused by a KOH activation burn-off phenomenon [15].

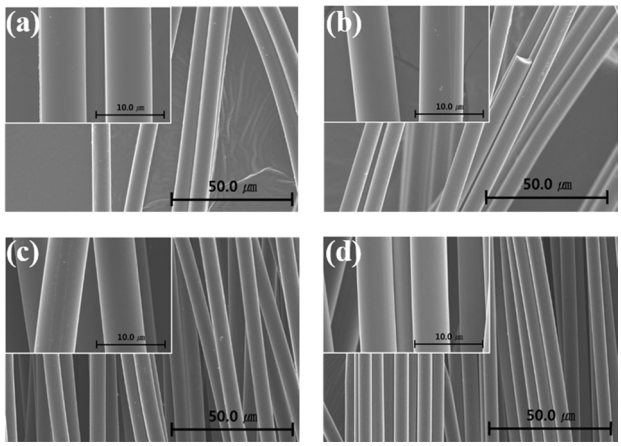

Fig. 1. FE-SEM images of (a) LCF, (b) 2K-LACF, (c) 4K-LACF, and (d) 6K-LACF samples.

The nitrogen adsorption/desorption isotherms of the LCFs and LACFs are presented in Fig. 2a. The relative pressure (P/P_0) of the non-activated LCF sample was almost constant despite absorption of an increasing quantity, which indicated a nonporous material. In contrast, the adsorption of the KOH-activated samples steeply increased below 0.05 P/P_0 and was constant above 0.05 P/P_0. A drastic increase in the adsorbed quantity below a certain relative pressure (P/P_0) and a constant value at the end of the isotherm typically indicate a microporous structure, which is designated as a Type I profile [16]. Type I profiles mainly show a powerful adsorption intensity or an absorbent with a micropore volume [17]. Therefore, 2K-LACF, 4K-LACF, and 6K-LACF were presumed to be similar microporous materials. The micropore volume and BET specific surface area of the 4K-LACF sample were expected to be the highest based on the initial adsorbed quantity and total quantity of adsorbed nitrogen.

Fig. 2b shows the pore-size distributions of LCFs and LACFs that were investigated using the density functional theory (DFT) method according to N_2 adsorption at 77 K. As expected from the nitrogen adsorption/desorption isotherms, all of the LACFs

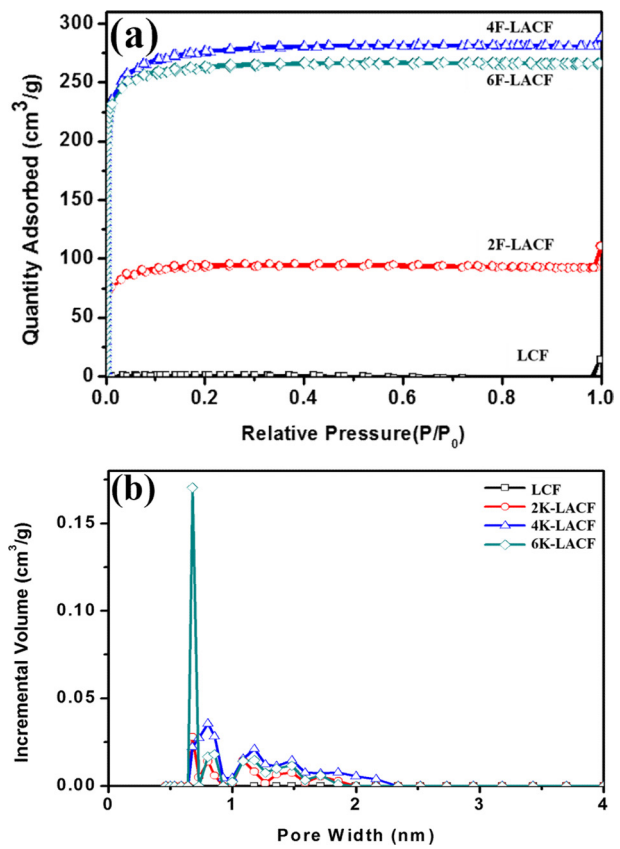

Fig. 2. Textural properties of LCFs and LACFs: (a) nitrogen isotherms and (b) pore-size distributions of LCFs and LACFs obtained by the DFT method.

Table 1. Textural properties of LCFs and LACFs

Sample	S_s (m^2 g^{-1})[a]	V_t (cm^3 g^{-1})[b]	V_{mic} (cm^3 g^{-1})[c]	V_{mes} (cm^3 g^{-1})[d]
LCF	5	0.14	-	-
2K-LACF	352	0.22	0.14	-
4K-LACF	1060	0.43	0.43	-
6K-LACF	1029	0.41	0.40	0.01

[a]BET specific surface area.
[b]Total pore volume.
[c]Micropore volume.
[d]Mesopore volume.

had a micropore volume. All samples showed an irregular pore-size distribution below 2.3 nm after the KOH chemical activation. In the process of KOH chemical activation, micro-channels develop vertically upon chemical attack by KOH, resulting in such a pore-size distribution [18]. In the 6K-LACF sample, the micropore volume of 0.6 to 0.7 nm was large (0.17 cm^3 g^{-1}), but the micropore volume of 0.5 to 2 nm was smaller than that of the 4K-LACF sample. Table 1 provides the detailed textural properties of the prepared samples. The BET specific surface areas and total pore volumes of the KOH-ACFs were 352 to 1060 m^2 g^{-1} and 0.22 to 0.43 cm^3 g^{-1}, respectively. The BET specific surface areas of the 4K-LACF and 6K-LACF samples were more than 1000 m^2 g^{-1} larger than that of the 2K-LACF sample. The KOH activation reaction with carbon materials is represented as follows (Eq. 1):

$$6KOH + C \leftrightarrow 2K + 3H_2 + 2K_2CO_3 \quad (1)$$

This reaction is followed by the decomposition of K_2CO_3 and the reaction of $K/K_2CO_3/CO_2$ with carbon materials [19,20]. Carbon materials can be oxidized by KOH, and the BET specific surface area and total pore volume increase due to the increasing micropore volume. Therefore, the BET specific surface area and total pore volume of the KOH-ACFs should increase as the KOH concentration increases. However, the BET specific surface and total pore volumes of 6K-LACF slightly decreased in comparison with those of 4K-LACF. This is because potassium can infiltrate the interior of the carbon structure and facilitate activation via the interaction of potassium with carbon [21], and this phenomenon is attributed to a micropore-merging effect. Micropores can be merged by the generation of carbon monoxide or carbon dioxide in the presence of an excess concentration of KOH [22].

Fig. 3 shows the CV plots of the LACFs obtained at scan rates of 5 and 50 mA s^{-1}. Because non-ACFs are a nonporous material, we excluded the CV plots of the LCF sample. Inclined rectangular and leaf-like CV curve shapes were observed due to the influence of the ohmic resistance, which was induced by electrolyte motion in the fiber pores during double-layer formation [23,24]. All of the electrodes exhibited inclined rectangular CV shapes with redox reaction peaks at 0.3 to 0.4 V, which indicated the occurrence of a pseudo-faradaic reaction caused by O functional groups at 5 mV s^{-1}, as shown in Fig. 3a [25,26]. Oxygen functional groups, such as ether/hydroxyl, carbonyl, and carboxyl groups, were introduced on the carbon surface via

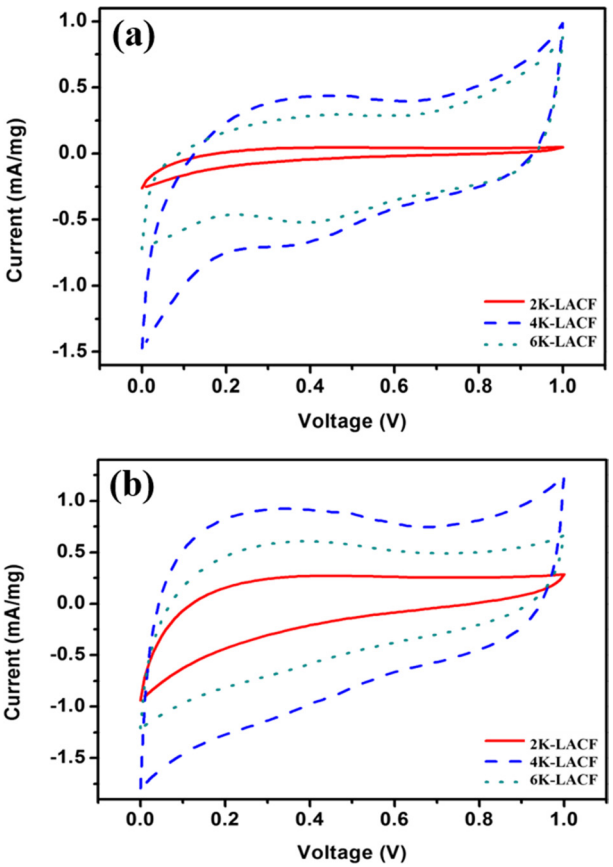

Fig. 3. Cyclic voltammograms of KOH-activated carbon fiber electrodes at (a) 5 mV s 1 and (b) 50 mV s 1.

KOH chemical activation [24]. Additionally, the intensity of the redox reaction peaks increased as the KOH concentration increased [25].

The specific discharge capacitances (C; F g^{-1}) of the LACF electrodes were calculated by [27]

$$C = \frac{1}{w\Delta V}\int_0^1 i\,dt \quad (2)$$

where C is the specific capacitance of the cell in F g^{-1}, w is the mass of the active material, i is the current flow for time dt, and ΔV is the potential window in which the current flows. The calculated specific capacitance of the LCFs was 0 F g^{-1} at both 5 and 50 mV s^{-1} due to their nonporous property. Additionally, the calculated specific capacitances were 24 and 3 F g^{-1} for 2K-LACF, 159 and 148 F g^{-1} for 4K-LACF, and 121 and 112 F g^{-1} for 6K-LACF at 5 and 50 mV/s, respectively. The specific capacitances increased with increasing KOH concentration, except for the 6K-LACF sample. This phenomenon is attributed to the BET specific surface areas and the total pore volumes of the activated samples increasing with the KOH concentration. Moreover, the well-developed micropore volume of 0.5 to 2.0 nm in 4K-LACF resulted in a higher specific capacitance than that of 0.6 to 0.7 nm in 6K-LACF.

To prepare LACFs, heat treatment and KOH chemical activation of carbon fibers were conducted. The diameter of the LACFs

gradually decreased as the KOH concentration and number of surface oxygen functional groups increased. The BET specific surface areas and micropore volumes of the LACFs ranged from 352 to 1060 m^2 g^{-1} and from 0.22 to 0.43 cm^3 g^{-1}, respectively. Due to the micropore-merging effect, the BET specific surface area and micropore volume of samples treated with excess KOH decreased. The EDLC performance was enhanced with 4 M KOH-activated LCFs, and these samples showed a specific capacitance of 159 and 121 F g^{-1} at scan rates of 5 and 50 mV s^{-1}, respectively. These results may be attributed to the increased BET specific surface area and total pore volume obtained at this KOH concentration. Additionally, the results indicate that a micropore volume of 0.5 to 2.0 nm is more effective than that of 0.6 to 0.7 nm for higher specific capacitances. In conclusion, an appropriate KOH treatment to induce a higher BET specific surface area and total pore volume is a crucial factor in preparing electrode materials for EDLCs.

Conflict of Interest

No potential conflict of interest relevant to this article was reported.

References

[1] Lei C, Markoulidis F, Ashitaka Z, Lekakou C. Reduction of porous carbon/Al contact resistance for an electric double-layer capacitor (EDLC). Electrochim Acta, **92**, 183 (2013). https://doi.org/10.1016/j.electacta.2012.12.092.

[2] Choi PR, Kim SG, Jung JC, Kim MS. High-energy-density activated carbon electrode for organic electric-double-layer-capacitor using carbonized petroleum pitch. Carbon Lett, **22**, 70 (2017). https://doi.org/10.5714/CL.2017.22.070.

[3] Jung MJ, Jeong E, Lee SI, Lee YS. Improved capacitance characteristics of activated carbon-based electrodes by physicochemical base-tuning. J Ind Eng Chem, **18**, 642 (2012). https://doi.org/10.1016/j.jiec.2011.11.055.

[4] Pandolfo AG, Hollenkamp AF. Carbon properties and their role in supercapacitors. J Power Sources, **157**, 11 (2006). https://doi.org/10.1016/j.jpowsour.2006.02.065.

[5] Kim J, Byun SC, Chung S, Kim S. Preparation and capacitance properties of graphene based composite electrodes containing various inorganic metal oxides. Carbon Lett, **25**, 14 (2018). https://doi.org/10.5714/CL.2018.25.014.

[6] Hirunpraditkoon S, Tunthong N, Ruangchai A, Nuithitikul K. Adsorption capacities of activated carbons prepared from bamboo by KOH activation. Int J Chem Mol Eng, **5**, 477 (2011).

[7] Bonnefoi L, Simon P, Fauvarque JF, Sarrazin C, Dugast A. Electrode optimisation for carbon power supercapacitors. J Power Sources, **79**, 37 (1999). https://doi.org/10.1016/S0378-7753(98)00197-9.

[8] Gopiraman M, Saravanamoorthy S, Kim SH, Chung IM. Interconnected meso/microporous carbon derived from pumpkin seeds as an efficient electrode material for supercapacitors. Carbon Lett, **24**, 73 (2017). https://doi.org/10.5714/CL.2017.24.73.

[9] Yoon SH, Lim S, Song Y, Ota Y, Qiao W, Tanaka A, Mochida I. KOH activation of carbon nanofibers. Carbon, **42**, 1723 (2004). https://doi.org/10.1016/j.carbon.2004.03.006.

[10] Endo M, Kim YJ, Ohta H, Ishii K, Inoue T, Hayashi T, Nishimura Y, Maeda T, Dresselhaus MS. Morphology and organic EDLC applications of chemically activated AR-resin-based carbons. Carbon, **40**, 2613 (2002). https://doi.org/10.1016/s0008-6223(02)00191-4.

[11] Nakagawa K, Mukai SR, Tamura K, Tamon H. Mesoporous activated carbons from phenolic resins. Chem Eng Res Des, **85**, 1331 (2007). https://doi.org/10.1205/cherd06119.

[12] Wang H, Zhong Y, Li Q, Yang J, Dai Q. Cationic starch as a precursor to prepare porous activated carbon for application in supercapacitor electrodes. J Phys Chem Solid, **69**, 2420 (2008). https://doi.org/10.1016/j.jpcs.2008.04.034.

[13] Albrecht W, Reintjes M, Wulfhorst B. Lyocell fibers (alternative regenerated cellulose fibers). Chem Fibers Int, **47**, 298 (1997).

[14] Wu QL, Gu SY, Gong JH, Pan D. SEM/STM studies on the surface structure of a novel carbon fiber from lyocell. Synth Met, **156**, 792 (2006). https://doi.org/10.1016/j.synthmet.2006.04.007.

[15] Lee D, Cho S, Kim Y, Lee YS. Influence of the pore properties on carbon dioxide adsorption of PAN-based activated carbon nanofibers. Polymer (Korea), **37**, 592 (2013). https://doi.org/10.7317/pk.2013.37.5.592.

[16] Jung MJ, Jeong E, Kim Y, Lee YS. Influence of the textual properties of activated carbon nanofibers on the performance of electric double-layer capacitors. J Ind Eng Chem, **19**, 1315 (2013). https://doi.org/10.1016/j.jiec.2012.12.034.

[17] Yoo HM, Min BG, Lee KH, Byun JH, Park SJ. Effect of KOH activation on electrochemical behaviors of graphite nanofibers. Polymer (Korea), **36**, 321 (2012). https://doi.org/10.7317/pk.2012.36.3.321.

[18] Lillo-Ródenas MA, Cazorla-Amorós D, Linares-Solano A. Understanding chemical reactions between carbons and NaOH and KOH: an insight into the chemical activation mechanism. Carbon, **41**, 267 (2003). https://doi.org/10.1016/s0008-6223(02)00279-8.

[19] Zhu Y, Murali S, Stoller MD, Ganesh KJ, Cai W, Ferreira PJ, Pirkle A, Wallace RM, Cychosz KA, Thommes M, Su D, Stach EA, Ruoff RS. Carbon-based supercapacitors produced by activation of graphene. Science, **332**, 1537 (2011). https://doi.org/10.1126/science.1200770.

[20] Im JS, Kang SC, Lee SH, Lee YS. Improved gas sensing of electrospun carbon fibers based on pore structure, conductivity and surface modification. Carbon, **48**, 2573 (2010). https://doi.org/10.1016/j.carbon.2010.03.045.

[21] Im JS, Park SJ, Lee YS. Superior prospect of chemically activated electrospun carbon fibers for hydrogen storage. Mater Res Bull, **44**, 1871 (2009). https://doi.org/10.1016/j.materresbull.2009.05.010.

[22] Jung MJ, Jeong E, Cho S, Yeo SY, Lee YS. Effects of surface chemical properties of activated carbon modified by amino-fluorination for electric double-layer capacitor. J Colloid Interface Sci, **381**, 152 (2012). https://doi.org/10.1016/j.jcis.2012.05.031.

[23] Mitani S, Lee SI, Saito K, Korai Y, Mochida I. Contrast structure and EDLC performances of activated spherical carbons with medium and large surface areas. Electrochim Acta, **51**, 5487 (2006). https://doi.org/10.1016/j.electacta.2006.02.040.

[24] Frackowiak E, Béguin F. Carbon materials for the electrochemical storage of energy in capacitors. Carbon, **39**, 937 (2011). https://doi.org/10.1016/s0008-6223(00)00183-4.

[25] Gupta V, Miura N. Polyaniline/single-wall carbon nanotube (PANI/SWCNT) composites for high performance supercapacitors. Electrochem Acta, **52**, 1721 (2006). https://doi.org/10.1016/j.electacta.2006.01.074.

[26] Tan PH, Hu CY, Li F, Bai S, Hou PX, Cheng HM. Intensity and profile manifestation of resonant raman behavior of carbon nanotubes. Carbon, **40**, 1131 (2002). https://doi.org/10.1016/s0008-6223(01)00261-5.

[27] Cho E, Bai BC, Im JS, Lee CW, Kim S. Pore size distribution control of pitch-based activated carbon for improvement of electrochemical property. J Ind Eng Chem, **35**, 341 (2016). https://doi.org/10.1016/j.jiec.2016.01.012.